The Methylamine Analogues of Wolffram's Red and Reihlen's Green: Syntheses, Infrared, Electronic, Raman, and Resonance-Raman Spectroscopy, and *X*-Ray Crystal Structures of Chain Chlorine- and Bromine-bridged Platinum(II,IV) Complexes of Methylamine†

Robin J. H. Clark* and Vincent B. Croud
Christopher Ingold Laboratories, University College London, 20 Gordon Street, London WC1H 0AJ
Helen M. Dawes and Michael B. Hursthouse
Department of Chemistry, Queen Mary College, Mile End Road, London E1 4NS

The syntheses and the electronic, i.r., Raman, and resonance-Raman spectra of the mixed-valence chain complexes $[Pt(CH_3NH_2)_4][Pt(CH_3NH_2)_4X_2][ClO_4]_4$, where X = Cl or Br, are reported. The electronic spectra are characterised by intense, broad intervalence bands whose maxima are at 24 100 and 18 200 cm^{-1}, respectively. The i.r. spectra are near superpositions of those of the constituent ions. The resonance-Raman spectra are dominated by long overtone progressions in ν_1, the symmetric X–Pt^{IV}–X stretch, of up to nine members for X = Cl and seven for X = Br. The ω_1 and x_{11} values for each complex are 324.8 ± 0.5 and −0.91 ± 0.07 cm^{-1}, respectively, for X = Cl and 186.3 ± 0.4 and −0.14 ± 0.1 cm^{-1} for X = Br. The Pt^{IV}–X stretching force constants are 2.08 and 1.55 mdyn $Å^{-1}$ for X = Cl and Br, respectively, and the X–Pt^{IV}–X interaction constants are 0.074 and 0.057 mdyn $Å^{-1}$, respectively. The excitation profiles for the ν_1 bands maximise 1 500—2 800 cm^{-1} to the red of the $Pt^{II} \longrightarrow Pt^{IV}$ intervalence band, as determined by transmission measurements. The crystal structures of the two complexes have been determined by single-crystal *X*-ray methods. In the bromide the structure contains ordered $[\cdots Pt^{II}(CH_3NH_2)_4 \cdots\cdots Br{-}Pt^{IV}(CH_3NH_2)_4{-}Br \cdots\cdots]$ chains; the Pt^{IV}–Br and Pt^{II}–Br distances are 2.468(3) and 3.219(4) Å, respectively, and the Pt^{II}–Br–Pt^{IV} angle is 165.4(3)°. The chloride structure contains an antiparallel disordering of the type of chain found in the bromide. The Pt^{IV}–Cl and Pt^{II}–Cl distances are 2.334(12) and 3.203(18) Å, respectively, and the Pt^{II}–Cl–Pt^{IV} angle is 170.5(6)°. Both the spectroscopic and the crystallographic evidence indicate that the platinum-ion valences are localised in these complexes.

Amine complexes of platinum have long been the subject of study, one of the best known being Wolffram's red, first prepared in 1900.[1] Although originally thought to be a complex of platinum(III), it is now well known to be the prototype mixed-valence chlorine-bridged chain complex, $[Pt(EtNH_2)_4][Pt(EtNH_2)_4Cl_2]Cl_4{\cdot}4H_2O$, with the structure shown below

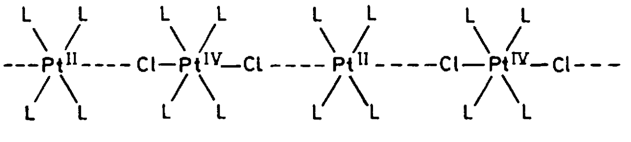

where L = ethylamine.[2] The analogous bromo-bridged species, known as Reihlen's green,[3] was first prepared in 1934. Although many similar complexes have since been prepared,[4,5] notably where L = NH_3, L–L = bidentate amine (many examples), and L–L–L = terdentate amine, the methylamine analogues had, until now, defied synthesis. On investigation, the principal difficulty was found to lie with the high solubility in water of both the constituent monomers as well as (by dissociation) any mixed-valence products. These difficulties have now been overcome, and the methylamine analogues of both Wolffram's red and Reihlen's green synthesised. The syntheses and properties of these complexes are reported in this paper, together with the electronic, i.r., Raman, and resonance-Raman spectroscopy of the complexes. Moreover, the *X*-ray crystal structures of both complexes are also described.

Experimental

Preparations of the Complexes.—Monomers. The complex $[Pt(CH_3NH_2)_4]Cl_2$ was prepared by the method of Watt *et al.*[6] The complexes $[Pt(CH_3NH_2)_4Br_2]Br_2$ and $[Pt(CH_3NH_2)_4Cl_2]Cl_2$ were obtained by oxidation of the parent platinum(II) species with dihalogen in water.

Mixed-valence complexes. Stoicheiometric quantities of the platinum monomers (*ca.* 0.5 g) and $Na[ClO_4]$ were dissolved in water (*ca.* 30 cm^3) and the volume slowly reduced to *ca.* 5 cm^3 on a steam-bath. The solution was then cooled and placed in a test tube in a vacuum desiccator containing silica gel until crystals appeared. The complexes are very soluble in water, in which they dissociate, and crystals of sodium perchlorate as well as of the unreacted monomers often contaminate the product. Therefore repeated recrystallisations are necessary.

The bromide forms either as red microcrystals or green metallic blades, the chloride as yellow microcrystals, orange-red crystals, or orange needles. The crystals were washed quickly with ice-cold water, ethanol, and acetone and dried in air. The chloride turns a flaxen colour on being dried.

An alternative method of purification is as follows. The impure solid was placed on a sinter and washed with diethyl ether (*ca.* 2 cm^3). The washings were discarded. Then the minimum amount of acetone was added to the crystals on the sinter under vacuum until they dissolved, leaving mainly perchlorate impurity behind on the sinter. The filtrate was then

---

† *Supplementary data available* (No. SUP 56400, 13 pp.): thermal parameters, H-atom co-ordinates, additional atom separations and angles. See Instructions for Authors, *J. Chem. Soc., Dalton Trans.*, 1986, Issue 1, pp. xvii—xx. Structure factors are available from the editorial office.

Non-S.I. unit employed: dyn = 10^{-5} N.

Table 1. Crystal data and details of structure analyses

Complex	$[Pt(CH_3NH_2)_4]$-$[Pt(CH_3NH_2)_4Br_2][ClO_4]_4$	$[Pt(CH_3NH_2)_4]$-$[Pt(CH_3NH_2)_4Cl_2][ClO_4]_4$
M	1 196.15	1 107.24
Crystal system	Monoclinic	Orthorhombic
a/Å	11.284(6)	9.932(4)
b/Å	15.675(4)	11.037(3)
c/Å	8.941(3)	14.991(4)
β/°	97.22(3)	
U/Å^3	1 569.0	1 643.4
Space group	$P2_1/c$	$Pnma$
Z	2	2
D_c/g cm^{-3}	2.533	2.382
$F(000)$	1 132	1 060
μ(Mo-K_α)/cm^{-1}	114.44	86.92
Crystal size/mm	0.38 × 0.08 × 0.01	0.51 × 0.13 × 0.10
θ range/°	1.5—25	1.5—25
Total unique data	2 760	1 523
Observed data	1 962	750
Significance test	$F_o > 3\sigma(F_o)$	$F_o > 3\sigma(F_o)$
No. of parameters	255	126
Coefficient g in weighting scheme $w = 1/[\sigma^2(F_o) + gF_o^2]$	0.000 25	0.0002
Final $R = \Sigma\Delta F/\Sigma F_o$	0.0369	0.0509
$R' = (\Sigma w\Delta F^2/\Sigma wF_o^2)^{\frac{1}{2}}$	0.0427	0.0608

Table 2. Properties of the complexes

Complex	Colour		Intervalence maximum[a]/cm^{-1}	E.p. maximum/cm^{-1}	ω_1/cm^{-1}	x_{11}/cm^{-1}	$I(2\nu_1)/I(\nu_1)$	Progression length
	crystal	powder						
$[Pt^{II}(CH_3NH_2)_4]$-$[Pt^{IV}(CH_3NH_2)_4Cl_2]$-$[ClO_4]_4$	Red-orange[b]	Yellow	24 100	*ca.* 21 250	324.8 ± 0.5	−0.91 ± 0.07	0.68 (457.9 nm)	$9\nu_1$ (457.9 nm)
$[Pt^{II}(CH_3NH_2)_4]$-$[Pt^{IV}(CH_3NH_2)_4Br_2]$-$[ClO_4]_4$	Metallic green	Red	18 200	*ca.* 16 700	186.3 ± 0.4	−0.14 ± 0.1	0.46 (520.8 nm)	$7\nu_1$ (520.8 nm)

[a] Nujol mull. [b] Crystals turn a flaxen colour when placed in a desiccator.

transferred to a beaker, and diethyl ether slowly added dropwise, with shaking, until the complex ceased to precipitate. The solid was filtered off and dried in air (Found: C, 8.40; H, 3.40; Cl, 19.35; N, 10.05. $C_4H_5Cl_3N_4O_8Pt$ requires C, 8.65; H, 3.65; Cl, 19.2; N, 10.1. Found: C, 7.45; H, 3.10; Br + Cl, 25.0; N, 8.65. $C_4H_5BrCl_2N_4O_8Pt$ requires C, 8.05; H, 3.35; Br + Cl, 25.2; N, 9.35%).

No analogous iodide-bridged complex could be prepared. A black insoluble solid, thought to be a platinum iodide, was invariably formed instead by the methods successfully used for the synthesis of the analogous chloro- and bromo-species. Moreover, the iodide-bridged complex could not be prepared by grinding the chloride with KI.

Instrumental Methods.—Electronic spectra were recorded at 295 K on a Cary 14 spectrometer. Samples were made up as Nujol mulls between quartz plates.

Infrared spectra were recorded on a Bruker IFS 113V interferometer. Spectra of each complex as wax discs were recorded in the region 700—20 cm^{-1} at *ca.* 80 K with use of an RIIC liquid-nitrogen cryostat. Spectra in the region 3 500—700 cm^{-1} were recorded for Nujol mulls between CsI plates at room temperature. Alkali-metal halide discs were not used due to the possibility of halogen exchange between the complex and the disc material.

Raman spectra were recorded on a Spex 1401 and on a Spex 14018/R6 spectrometer. Exciting radiation was provided by Coherent models CR3, CR500 K, and CR3000 K lasers. Samples were held in the forms of pressed discs of the complex dispersed in dried $K_2[SO_4]$ or $K[ClO_4]$. A Dewar assembly using liquid nitrogen was used for measurements at *ca.* 80 K and an Air Products Displex cryostat for those at *ca.* 10 K. Spectra were calibrated by reference to the emission spectra of neon or to the Rayleigh line. Excitation profiles (e.p.s) were recorded for samples held at *ca.* 80 K, with the a_1 band of $[SO_4]^{2-}$ as internal intensity standard. Intensities were corrected for the spectral response of each instrument.

X-Ray Crystallography.—Crystals of the bromide were thin elongated plates; a section of one was cut and transferred to a Lindemann capillary while immersed in mother-liquor. Oscillation photographs revealed the $h = 2n + 1$ layers to be weak but with well defined sharp spots. Repeated recrystallisations of the chloride gave only extremely thin, fragile orange needles. *X*-Ray photography indicated most specimens to be twinned. Eventually a single specimen was obtained, and mounted with a coating of mother-liquor in a Lindemann capillary. Although the specimen was seen to contain a hair-line fracture along the needle axis, it proved to be useable for data collection, which was carried out at 265 K.

Intensity data for both crystals were recorded on a Nonius CAD4 diffractometer using Mo-K_α radiation and an ω–2θ

Table 3. Fractional atomic co-ordinates (× 10^4)

Atom	*x*	*y*	*z*	Atom	*x*	*y*	*z*
(*a*) $[Pt(CH_3NH_2)_4][Pt(CH_3NH_2)_4Br_2][ClO_4]_4$							
Pt(1)	0	0	0	Cl(1)	−2 544(2)	−2 046(2)	5 866(3)
Pt(2)	5 000	0	0	Cl(2)	−2 346(2)	1 071(2)	4 601(3)
Br	2 189(1)	−178(1)	248(1)	O(11)	−2 618(6)	−2 964(4)	5 867(8)
N(11)	40(7)	−90(5)	2 314(9)	O(12)	−1 386(7)	−1 796(5)	6 571(10)
C(11)	−515(9)	−835(6)	2 971(10)	O(13)	−2 705(8)	−1 763(5)	4 361(9)
N(12)	410(6)	1 280(4)	341(7)	O(14)	−3 444(8)	−1 704(5)	6 664(9)
C(12)	−530(9)	1 931(6)	179(12)	O(21)	−2 181(9)	224(6)	5 144(12)
N(21)	5 675(7)	−516(5)	2 047(8)	O(22)	−1 455(7)	1 247(5)	3 667(9)
C(21)	4 805(9)	−669(7)	3 128(11)	O(23)	−2 217(7)	1 595(6)	5 855(10)
N(22)	4 806(6)	1 167(5)	1 003(8)	O(24)	−3 503(7)	1 100(6)	3 839(10)
C(22)	5 597(9)	1 878(6)	542(12)				
(*b*) $[Pt(CH_3NH_2)_4][Pt(CH_3NH_2)_4Cl_2][ClO_4]_4$							
Pt(1)	0	0	0	Cl(3)	3 803(9)	2 500	1 155(7)
Cl(1)	−149(10)	2 105(9)	112(6)	O(11)	1 840(36)	2 500	6 490(9)
N(1)	−666(21)	253(20)	−1 282(13)	O(12)	507(17)	2 500	7 747(22)
C(1)	−272(22)	−586(24)	−1 965(13)	O(13)	2 583(13)	1 465(13)	7 822(12)
N(2)	1 973(17)	374(16)	−418(12)	O(21)	5 196(13)	2 500	1 441(16)
C(2)	2 859(23)	−617(26)	−496(20)	O(22)	3 829(39)	2 500	191(10)
Cl(2)	1 878(10)	2 500	7 444(6)	O(23)	3 187(18)	1 369(15)	1 358(17)

Table 4. Bond lengths (Å) and angles (°) for $[Pt(CH_3NH_2)_4][Pt(CH_3NH_2)_4Br_2][ClO_4]_4$

Pt(1)–Br	2.468(3)	Pt(2) · · · Br	3.219(4)
Pt(1)–N(11)	2.068(10)	Pt(1)–N(12)	2.073(9)
Pt(2)–N(21)	2.058(9)	Pt(2)–N(22)	2.061(9)
C(11)–N(11)	1.481(13)	C(12)–N(12)	1.466(13)
C(21)–N(21)	1.481(13)	C(22)–N(22)	1.517(14)
O(11)–Cl(1)	1.441(8)	O(12)–Cl(1)	1.432(8)
O(13)–Cl(1)	1.406(9)	O(14)–Cl(1)	1.418(9)
O(21)–Cl(2)	1.419(10)	O(22)–Cl(2)	1.413(9)
O(23)–Cl(2)	1.382(9)	O(24)–Cl(2)	1.396(9)
N(11)–Pt(1)–Br	90.4(3)	N(12)–Pt(1)–Br	83.9(3)
N(12)–Pt(1)–N(11)	86.7(4)	N(21)–Pt(2)–Br	99.3(3)
N(22)–Pt(2)–Br	83.6(3)	N(22)–Pt(2)–N(21)	90.5(4)
Pt(2)–Br–Pt(1)	165.4(3)	C(11)–N(11)–Pt(1)	119.5(6)
C(12)–N(12)–Pt(1)	121.0(7)	C(21)–N(21)–Pt(2)	116.3(7)
C(22)–N(22)–Pt(2)	115.8(6)	O(12)–Cl(1)–O(11)	108.8(6)
O(13)–Cl(1)–O(11)	108.4(6)	O(14)–Cl(1)–O(11)	109.3(6)
O(13)–Cl(1)–O(12)	109.6(6)	O(14)–Cl(1)–O(12)	110.3(6)
O(14)–Cl(1)–O(13)	110.4(6)	O(22)–Cl(2)–O(21)	108.2(7)
O(23)–Cl(2)–O(21)	106.4(7)	O(24)–Cl(2)–O(21)	105.8(7)
O(23)–Cl(2)–O(22)	110.7(6)	O(24)–Cl(2)–O(22)	113.3(7)
O(24)–Cl(2)–O(23)	111.9(7)		

Table 5. Bond lengths (Å) and angles (°) for $[Pt(CH_3NH_2)_4][Pt(CH_3NH_2)_4Cl_2][ClO_4]_4$

Pt(1)–Cl(1)	2.334(12)	Pt(1) · · · Cl(1^{I})	3.203(18)
Pt(1)–N(1)	2.051(21)	Pt(1)–N(2)	2.099(18)
C(1)–N(1)	1.435(29)	C(2)–N(2)	1.409(28)
O(11)–Cl(2)	1.431(10)	O(12)–Cl(2)	1.435(10)
O(13)–Cl(2)	1.454(10)	O(21)–Cl(3)	1.449(10)
O(22)–Cl(3)	1.445(11)	O(23)–Cl(3)	1.423(10)
N(1)–Pt(1)–Cl(1)	84.9(8)	N(2)–Pt(1)–Cl(1)	83.4(6)
N(2)–Pt(1)–N(1)	89.7(9)	Pt(1)–Cl(1)–Pt(1^{I})	170.5(6)
C(1)–N(1)–Pt(1)	119.5(15)	C(2)–N(2)–Pt(1)	117.1(16)
O(12)–Cl(2)–O(11)	106.9(23)	O(13)–Cl(2)–O(11)	113.7(13)
O(13)–Cl(2)–O(12)	109.5(12)	O(13)–Cl(2)–O(13^{II})	103.5(17)
O(22)–Cl(3)–O(21)	106.2(21)	O(23)–Cl(3)–O(21)	110.3(11)
O(23)–Cl(3)–O(22)	102.9(15)	O(23)–Cl(3)–O(23^{II})	122.6(22)

Key to symmetry operations relating designated atoms to reference atoms at (*x*,*y*,*z*): I $-x$, $0.5 + y$, $-z$; II x, $0.5 - y$, z.

scan.[7] The ω-scan angle for the chloride complex was increased to allow for the broader peaks. Both data sets were corrected for absorption empirically, a further adjustment being made during structure solution.[8] Crystal data for the complexes are presented in Table 1.

Solution and refinement of $[Pt(CH_3NH_2)_4][Pt(CH_3NH_2)_4Br_2][ClO_4]_4$. The Patterson synthesis was consistent with the location of two independent platinum atoms at inversion centres *a*/2 apart [assigned as (0,0,0) and (0.5,0,0)] in space group $P2_1/c$. A bromine atom was located at approximately (0.22,0,0). Difference maps revealed the positions of two methylamine ligands co-ordinated to each platinum atom together with two perchlorate anions. Refinement proceeded by full-matrix least squares [9] with anisotropic thermal parameters for all non-hydrogen atoms. Hydrogen atoms were included in the structure-factor calculation and refined using a damping factor [9] and assuming a common isotropic thermal parameter for those attached to a particular C or N atom.

Solution and refinement of $[Pt(CH_3NH_2)_4][Pt(CH_3NH_2)_4Cl_2][ClO_4]_4$. The crystal system was determined to be orthorhombic, with absences indicating the space group *Pnma* or $Pn2_1a$ (alternative to standard $Pna2_1$). Solution was attempted in space group *Pnma* with a platinum atom assigned to a centre of inversion at (0,0,0), a site for a chlorine atom appearing on the mirror plane at approximately (0,0.25,0). As with the bromide complex, two methylamine ligands were located, bonded to the metal atom. The chlorine atom which refines with a large U_{22} value when confined to the mirror plane is represented as disordered over two sites across this plane. The two independent perchlorate anions, for each of which the chlorine atom and two oxygen atoms lie at $y = \frac{1}{4}$ were, as with all other non-hydrogen atoms, refined with anisotropic thermal parameters. Hydrogen atoms were treated in the same manner as in the bromide complex. In order to achieve stable refinement, several of the C–H distances and perchlorate Cl–O distances were fixed.

We considered the possibility that the space group might be $Pn2_1a$ but discarded the idea for the following reasons. An

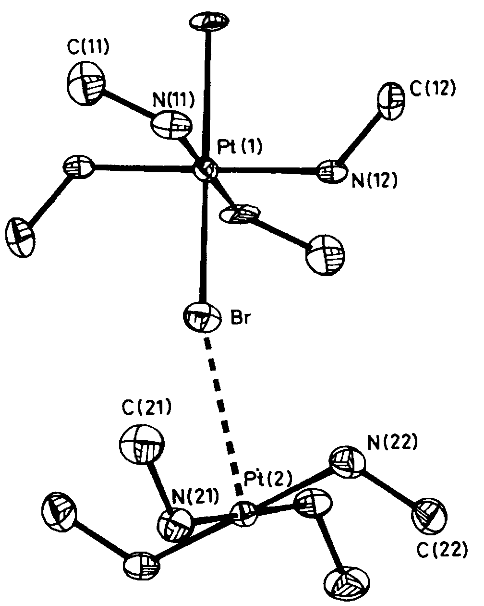

Figure 1. Co-ordination environment for the $[Pt(CH_3NH_2)_4][Pt(CH_3NH_2)_4Br_2]$ chain

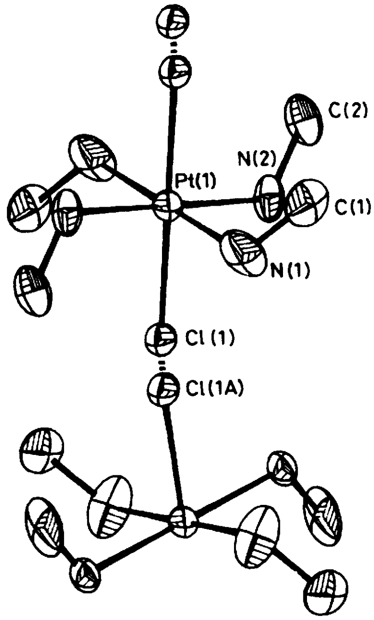

Figure 2. Co-ordination environment for the $[Pt(CH_3NH_2)_4][Pt(CH_3NH_2)_4Cl_2]$ chain

ordered chain along the 2_1 direction would require each Pt atom to be chemically equivalent and identifiable as five-co-ordinate Pt^{III}. The spectroscopic results are not consistent with this. The refinement in the centrosymmetric space group proceeded without problems; there is no serious disorder apart from the chloride positioning and some anisotropy in some (but not all) ClO_4 groups. More importantly, the $Pt(CH_3NH_2)_4$ units conform well to the required centrosymmetric arrangement. Finally, there are no indications of unacceptable 'non-bonded' contacts, a common occurrence in cases where the space-group symmetry is overestimated.

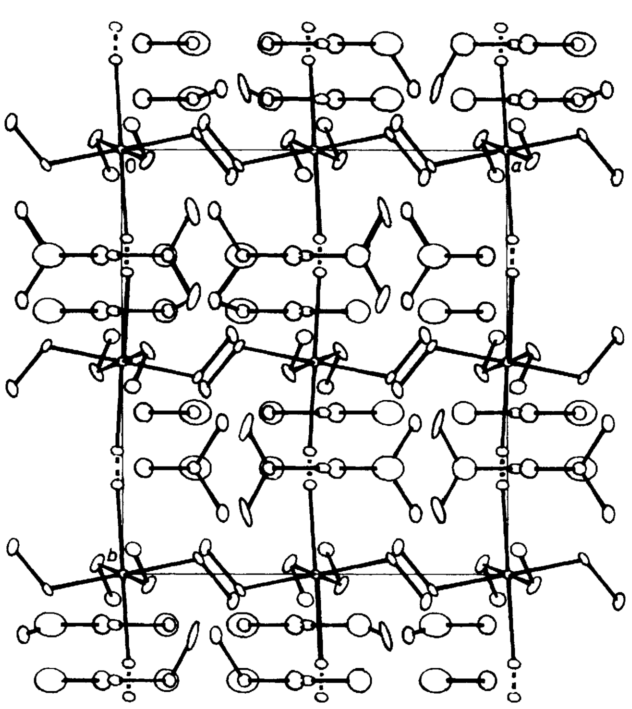

Figure 3. Packing diagram for the complex $[Pt(CH_3NH_2)_4][Pt(CH_3NH_2)_4Cl_2][ClO_4]_4$ (ellipsoids drawn at 10% probability)

Results and Discussion

The syntheses of the methylamine analogues of Wolffram's red and Reihlen's green have been successfully accomplished, the complexes forming as strongly coloured, dichroic needles (Table 2) with intervalence bands (by transmission through Nujol mulls) at 24 100 and 18 200 cm^{-1}, respectively. The synthetic work thus removes the oddity that both ammonia and ethylamine were known to form complexes of Pt^{II}/Pt^{IV} but, until now, not methylamine. All the physical properties of the methylamine complexes suggest that they are chain, halogen-bridged complexes; however, since it was not obvious whether or not the chains are linear, the *X*-ray structures of each complex were established.

X-Ray Structures.—Final fractional atomic co-ordinates are listed in Table 3, bond lengths and angles in Tables 4 and 5.

The structure of $[Pt(CH_3NH_2)_4][Pt(CH_3NH_2)_4Br_2][ClO_4]_4$ comprises an ordered octahedral platinum(IV) [Pt^{IV}–Br 2.468(3) Å] and square-planar platinum(II) [$Pt^{II}\cdots$Br 3.219(4) Å] chain arrangement of the type Br–Pt^{IV}–Br$\cdots$$Pt^{II}$ (see Figure 1). The chloride analogue however contains a disordered, antiparallel, arrangement of chains of the above type, with all platinum sites crystallographically equivalent and the chlorine atom half-occupying two adjacent sites between Pt atoms [Pt–Cl 2.334(12) and 3.203(18) Å] (see Figure 2).

In neither structure is the $Pt^{II}\cdots X\text{–}Pt^{IV}$ angle 180°, as is usual for this type of complex,[5] but is 165° for X = Br and 170° for X = Cl. In addition there is a near 20° twist (*cf.* 0° in Reihlen's green, 37° in anhydrous Reihlen's green)[10] of the $Pt^{II}L_4$ and $Pt^{IV}L_4$ units relative to one another, *i.e.* away from the eclipsed position in the bromide structure. In the chloride structure the groups are perfectly eclipsed since the two PtL_4 units are related by the mirror plane. The difference between the bromide and chloride structures probably arises from the small change in separation of the PtL_4 units in the Pt–Cl$\cdots$Pt and Pt–Br$\cdots$Pt linkages. This could then allow changes in the tilts of the PtN_4 planes, the bend of the Pt–X$\cdots$Pt angle, and the

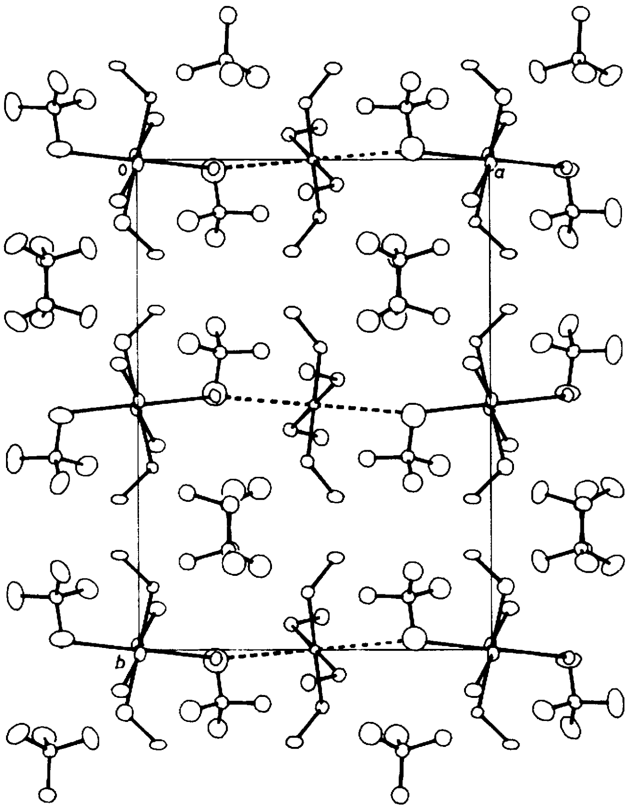

Figure 4. Packing diagram for the complex $[Pt(CH_3NH_2)_4][Pt(CH_3NH_2)_4Br_2][ClO_4]_4$ (ellipsoids drawn at 30% probability)

relative twists of the PtL_4 units, as the structures seek to accommodate steric interactions and hydrogen bonding. A number of contacts occur in each structure between perchlorate oxygen atoms and amine nitrogen atoms (O ··· N *ca.* 2.9—3.2 Å) and, although these are not strong, they almost certainly contribute to the stabilising of the crystal structures. (Packing diagrams for the two structures are given in Figures 3 and 4.) Such interactions may account for the fact that the platinum atoms are not in the plane of the nitrogen atoms (as is also the case for the analogous ethylamine complex).

The values of $r(M^{IV}-X)/r(M^{II}-X)$ (0.76 for X = Br, 0.73 for X = Cl) are lower than average for cation-chain platinum complexes,[5] indicating that the valences are fairly localised (see below). The fact that the interaction between the metal(II) and metal(IV) centres is relatively weak is probably due to the non-linearity of the $Pt^{II} \cdots X-Pt^{IV}$ unit.

The line group for both complexes is C_1.

Infrared Spectra.—The i.r. spectra of the mixed-valence complexes have been recorded at room temperature for the region 3 500—700 cm^{-1} and at *ca.* 80 K for the region 700—20 cm^{-1}. The band wavenumbers and assignments are given in Table 6. The spectra consist essentially of superpositions of the i.r. spectra of the constituent complexes as expected for fairly localised-valence complexes. Differences are expected to be due mainly to changes in the axial $Pt^{IV}-X$ force constant consequent upon interaction with the platinum(II) centre, to changes in amine modes due to hydrogen-bond formation, and to site and correlation splitting.

Table 6. Wavenumbers (cm^{-1}) and assignments of bands observed in the i.r. spectra of $[Pt^{II}(CH_3NH_2)_4][Pt^{IV}(CH_3NH_2)_4X_2][ClO_4]_4$

X = Cl[a]	X = Br[b]	Assignment
3 306 (sh)	3 310m	
3 277 (sh)	3 283m	
3 265s	3 258m	
3 224s	3 224m	ν(N–H)
3 183 (sh)	3 181m	
3 142s	3 151m	
	3 125 (sh)	
	3 052w	ν(C–H)
2 721vw		
	1 715vw	
1 598m	1 607m	δ(NH_2)
1 579 (sh)	1 582m	
1 511w	1 512w	
	1 412w	
	1 337w	
1 300m	1 301w	ω(NH_2)?
	1 284w	
	1 257w	
1 146s	1 136s	
	1 116 (sh)	
1 103s	1 094vs	γ(NH_2)
1 079 (sh)	1 076 (sh)	
	1 057s	ν(C–N)
	1 042 (sh)	
988m	989 (sh)	ρ(CH_3)
935w (sh)	936vw	
928w	930w	
757w	760w	
736w	738w	
722w		ρ(NH_2)
628vs	624m	$[ClO_4]^-$
528s	538m	
522s		
519 (sh)		ν(Pt–N)
514w		
510m	502m	
476w		
469w	457m	
453w	455 (sh)	
	453m	
	433br	
365.5s		ν_2, $\nu_{asym}(Cl-Pt^{IV}-Cl)$
364 (sh)		
	343 (sh)	
	340w	
	327m	
317vs	319 (sh)	
	312 (sh)	
305m	306s	
296s	288s	δ(NPtN)
282w	280s	
270s		
268 (sh)		
258s		
256 (sh)		
254s		
	238s	ν_2, $\nu_{asym}(Br-Pt^{IV}-Br)$
	236 (sh)	
	232 (sh)	

[a] Additional peaks observed at 193m, 185w, 164s, 148s, 125m, 123 (sh), 116 (sh), and 114s cm^{-1}. [b] Additional peaks observed at 194m, 184w, 181w, 164 (sh), 162s, 146w, 142 (sh), 125m, 123 (sh), 111m, 109w (sh), 106m, 99w, and 94w cm^{-1}.

The chlorine isotopic splitting of ν_2, $\nu_{asym.}(Cl-Pt^{IV}-Cl)$, was not fully resolved for $[Pt(CH_3NH_2)_4][Pt(CH_3NH_2)_4Cl_2][ClO_4]_4$, by contrast to the situation for many other related chain complexes of platinum.[11]

Resonance-Raman Spectra.—The spectra are shown in

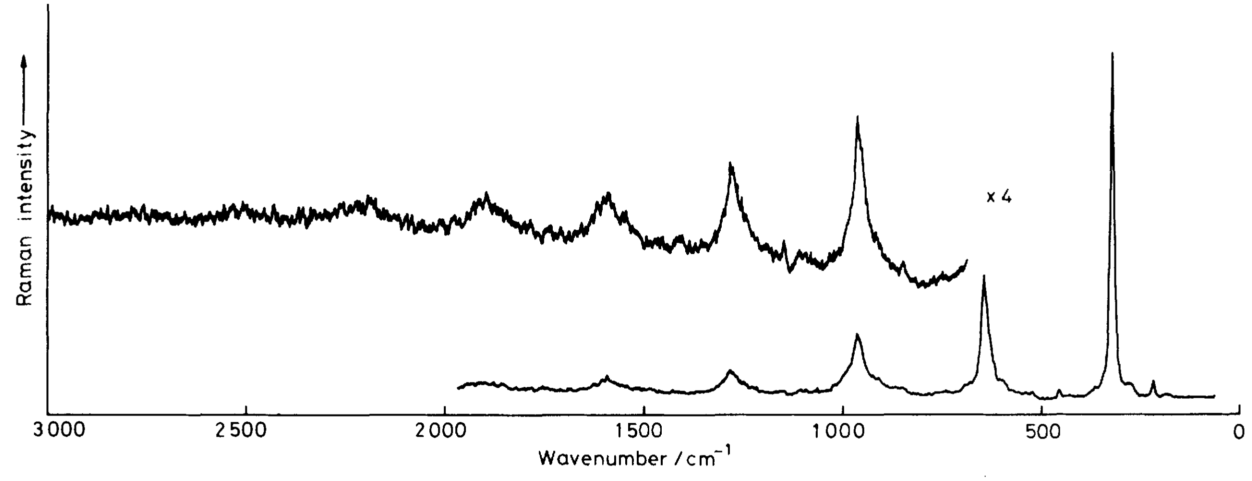

Figure 5. Resonance-Raman spectrum of $[Pt(CH_3NH_2)_4][Pt(CH_3NH_2)_4Cl_2][ClO_4]_4$ as a $K_2[SO_4]$ disc at *ca.* 80 K, λ_0 = 457.9 nm (slits 150, 200, and 150 μm)

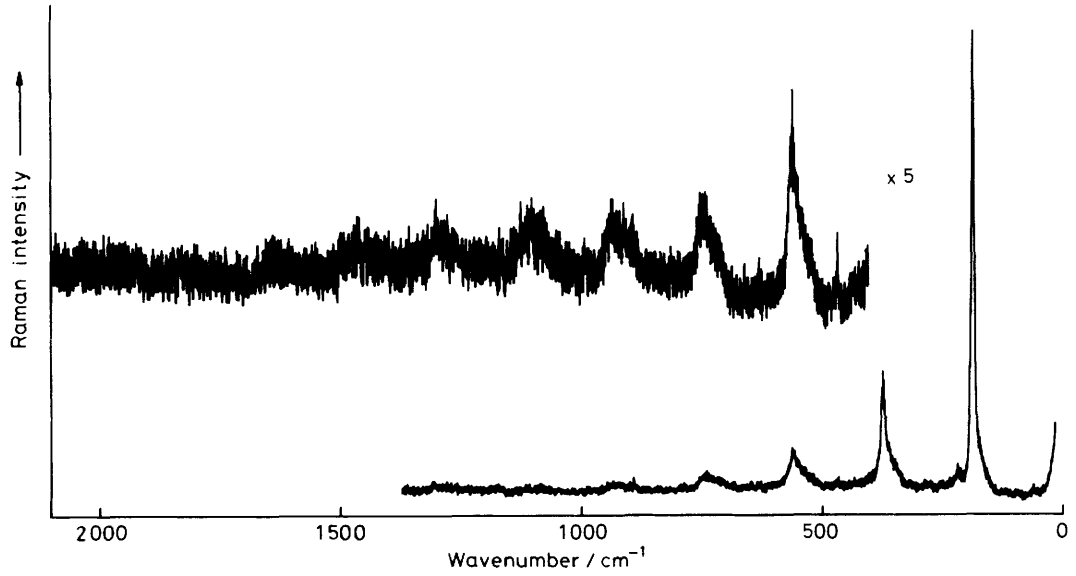

Figure 6. Resonance-Raman spectrum of $[Pt(CH_3NH_2)_4][Pt(CH_3NH_2)_4Br_2][ClO_4]_4$ as a $K[ClO_4]$ disc at *ca.* 80 K, λ_0 = 520.8 nm (slits 150, 200, and 150 μm)

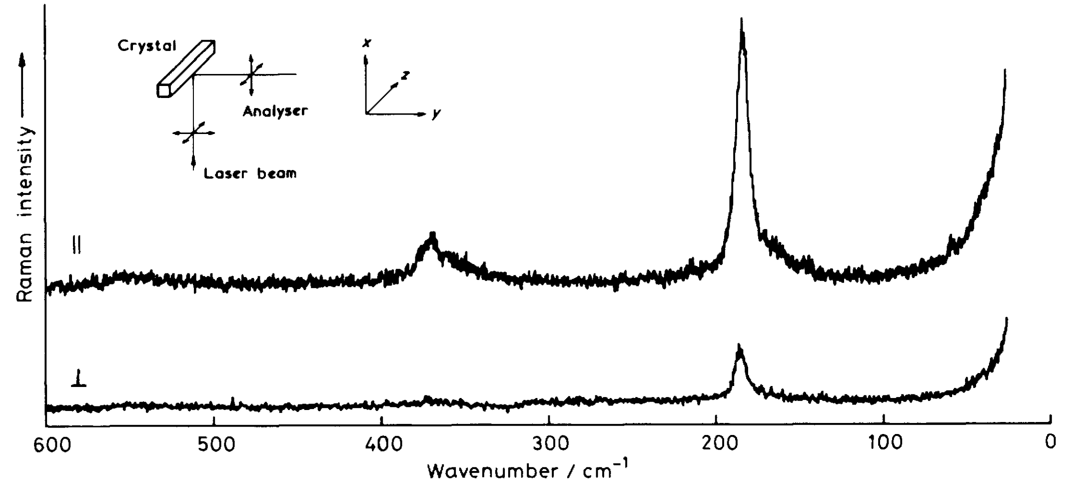

Figure 7. Polarised single-crystal spectrum of $[Pt(CH_3NH_2)_4][Pt(CH_3NH_2)_4Br_2][ClO_4]_4$, λ_0 = 520.8 nm; $x(zz)y$ = ||, $x(zx)y$ = ⊥

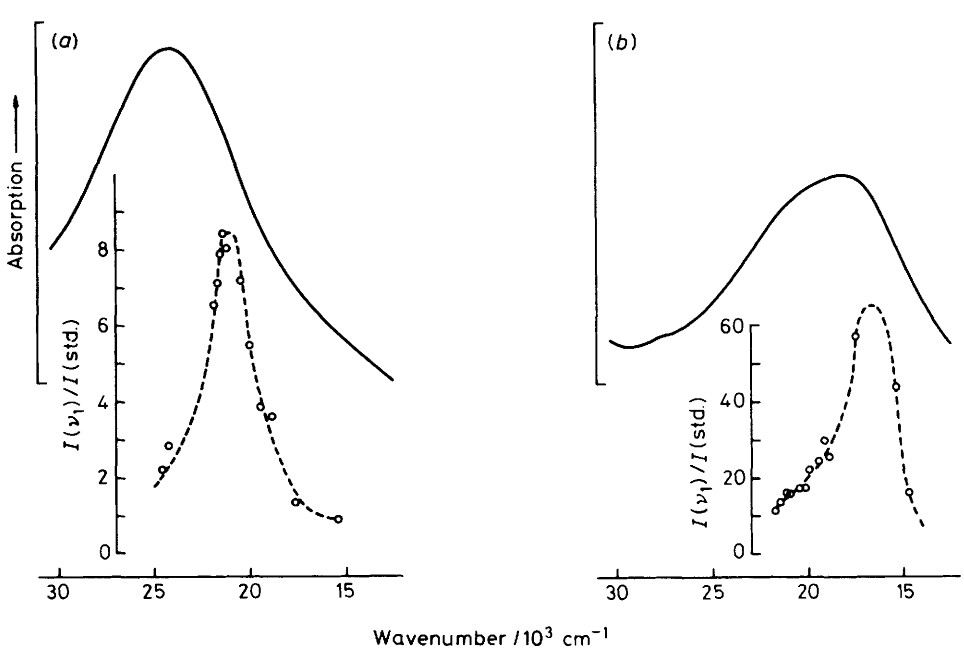

Figure 8. Electronic spectra (295 K) and excitation profiles (*ca.* 80 K) of the ν_1 band of (*a*) $[Pt(CH_3NH_2)_4][Pt(CH_3NH_2)_4Cl_2][ClO_4]_4$ and (*b*) $[Pt(CH_3NH_2)_4][Pt(CH_3NH_2)_4Br_2][ClO_4]_4$

Table 7. Wavenumbers, relative intensities, full widths at half-maximum, and assignments of bands observed in the resonance-Raman spectrum of $[Pt(CH_3NH_2)_4][Pt(CH_3NH_2)_4Br_2][ClO_4]_4$

$\tilde{\nu}$/cm^{-1}	$I(\upsilon_1\nu_1)/I(\nu_1)$	$\Delta\tilde{\nu}_{\frac{1}{2}}$/cm^{-1}	Assignment
60			ν_3?
93			δ(Br–Pt–N)
120			
173			
185.5	1	6.4	ν_1, ν_{sym}(Br–Pt^{IV}–Br)
217.1			δ(N–Pt–N)
248.6			ν_1 + 60
283			
345			2 × 173
372.5	0.46	12.8	2ν_1
437			2ν_1 + 60?
464			$[ClO_4]^-$
476			
487			
518			ν(Pt–N) or 3 × 173
534			ν(Pt–N)
548			
552			
558.4	0.32	28	3ν_1
629			
724.5			ν_1 + 534
742.9	0.11	40	4ν_1
902			2ν_1 + 534
925.5	0.08	48	5ν_1
940			$[ClO_4]^-$ or ρ(CH_3)
1 094			3ν_1 + 534
1 106.0	0.04	60	6ν_1
1 125			ν_1 + 940?
1 278	<0.04	>60	7ν_1

Recorded as $K[ClO_4]$ disc at *ca.* 80 K using 520.8-nm excitation and slit widths of 100, 150, and 100 μm (spectral slit width *ca.* 1 cm^{-1}).

Table 8. Wavenumbers, relative intensities, full widths at half-maximum, and assignments of bands observed in the resonance-Raman spectrum of $[Pt(CH_3NH_2)_4][Pt(CH_3NH_2)_4Cl_2][ClO_4]_4$

$\tilde{\nu}$/cm^{-1}	$I(\upsilon_1\nu_1)/I(\nu_1)$	$\Delta\tilde{\nu}_{\frac{1}{2}}$/cm^{-1}	Assignment
50.9vw			ν_3?
188.1			
218.2			δ(N–Pt–N)
275w,br			
317			
322.2	1.0	12	ν_1, ν_{sym}(Cl–Pt^{IV}–Cl)
349.1			
434			
463.8			$[ClO_4]^-$
524.3			ν(Pt–N)
539.4			
563.4			
596			
644.1	0.68	23	2ν_1
690.2			
744			ρ(NH_2)?
846.1			ν_1 + 524.3
916.8			ν_1 + 596
943			$[ClO_4]^-$
964.5	0.49	34	3ν_1
1 170			2ν_1 + 524.3
1 238			2ν_1 + 596
1 281	0.25	43	4ν_1
1 598	0.19	65	5ν_1
1 626			δ(NH_2)?
1 907	0.15	70	6ν_1
1 920			
2 215	0.13	98	7ν_1
2 516	<0.1	>98	8ν_1
2 802	<0.1	>98	9ν_1

Recorded as a $K[ClO_4]$ disc at *ca.* 80 K using 457.9-nm excitation and slit widths of 150, 200, and 150 μm (spectral slit width *ca.* 2.0 cm^{-1}).

Figures 5 and 6 and the wavenumbers and assignments of the observed bands are given in Tables 7 and 8. The resonance-Raman spectra are dominated by long overtone progressions in ν_1, the totally symmetric X–Pt^{IV}–X stretching mode (reaching $9\nu_1$ for X = Cl, $7\nu_1$ for X = Br). Subsidiary progressions, in particular $v_1\nu_1 + \nu(\text{PtN})$, are also apparent in the spectra of each complex. The long progressions in ν_1 imply a substantial elongation of the Pt^{IV}–X bonds in the intervalence state,[4] and the involvement of ν(PtN) in subsidiary progressions implies that there is a small consequential change to the PtN co-ordinate. This change would arise since elongation of the Pt^{IV}–X bonds could alter the extent of interaction (steric or electronic) between the amine methyl groups and the bridging halogen atoms.

The harmonic band wavenumbers ω_1, and anharmonicity constants x_{11}, derived from the resonance-Raman data, are listed in Table 2.

The single-crystal spectrum (Figure 7) of the bromide-bridged complex was found to be not completely chain (z) polarised, this being a consequence of the non-linearity of the chain.

It was not found possible to resolve the isotopic splitting for the ν_1 band of the chloride complex, even for a single crystal at *ca.* 10 K and low incident laser power. However, the ν_1 band is asymmetric to the low-wavenumber side and the asymmetry is more pronounced for the overtone bands. Approximate force constants have been calculated using a linear MX_2 model[11] on the assumption that the most intense metal–halogen peak arises from the ^{35}Cl–Pt^{IV}–^{35}Cl isotopomer for the chloride and from the ^{80}Br–Pt^{IV}–^{80}Br (mass average) species for the bromide. The results are: $f_r = 2.08, f_{rr} = 0.074$ mdyn Å^{-1} for the chloride, and $f_r = 1.55, f_{rr} = 0.057$ mdyn Å^{-1} for the bromide. The f_r values are significantly higher than for other platinum chain complexes,[11] implying that the platinum valences are more localised in methylamine than in other chain complexes.

No measureable wavenumber shift of ν_1 with exciting line was detected for either complex, consistent with their localised-valence nature.[12]

The bromide complex was destroyed when ground with K[NO$_3$], possibly due to the presence of trace amounts of water in the latter, and hence dry K$_2$[SO$_4$] or dry K[ClO$_4$] was used as matrix materials.

The excitation profiles of the ν_1 bands (Table 2, Figure 8) maximise to the red (by 2 800 and 1 500 cm^{-1} for the chloride and bromide, respectively) of the intervalence band maximum, as determined by transmission measurements. This is the typical behaviour of linear-chain complexes, for which the excitation profile appears to locate the absorption edge rather than the band maximum.

Conclusions

The new methylamine complexes are localised-valence species with an unusual arrangement of the equatorial amine groups and substantial chain bending at the bridging halogen atom (by 165.4—170.5°).

Acknowledgements

The authors thank the S.E.R.C. and Johnson Matthey Ltd. for financial assistance, and Dr. M. Kurmoo for useful discussions.

References

1 H. Wolffram, Dissertation, Königsberg, 1900.
2 B. M. Craven and D. M. Hall, *Acta Crystallogr.*, 1961, **14**, 475.
3 H. Reihlen and E. Flohr, *Ber.*, 1934, **67**, 2010.
4 R. J. H. Clark, *Chem. Soc. Rev.*, 1984, **13**, 219.
5 R. J. H. Clark in 'Advances in Infrared and Raman Spectroscopy,' eds. R. J. H. Clark and R. E. Hester, Wiley-Heyden, Chichester, 1984, vol. 11, p. 95.
6 G. W. Watt, B. B. Hutchinson, and D. S. Klett, *J. Am. Chem. Soc.*, 1967, **89**, 2007.
7 M. B. Hursthouse, R. A. Jones, K. M. A. Malik, and G. Wilkinson, *J. Am. Chem. Soc.*, 1979, **101**, 4128.
8 N. Walker and D. Stuart, *Acta Crystallogr., Sect. A*, 1983, **39**, 158.
9 G. M. Sheldrick, SHELX 76 program for crystal structure determination, University of Cambridge, 1976.
10 R. J. H. Clark and P. C. Turtle, *Inorg. Chem.*, 1978, **17**, 2526.
11 S. D. Allen, R. J. H. Clark, V. B. Croud, and M. Kurmoo, *Philos. Trans. R. Soc. London, Ser. A*, 1985, **314**, 131.
12 R. J. H. Clark and M. Kurmoo, *J. Chem. Soc., Faraday Trans. 2*, 1983, 519.

Received 25th March 1985; *Paper* 5/491